Influence of triplet instabilities in TDDFT

Michael J. G. Peach,* Matthew J. Williamson[a] and David J. Tozer[†]

Department of Chemistry, Durham University,
South Road, Durham, DH1 3LE UK.
Fax: +44 191 384 4737

* Email: M.J.G.Peach@Durham.ac.uk
[†] Email: D.J.Tozer@Durham.ac.uk

[a] Current address: School of Physics and Astronomy,
The University of Edinburgh, James Clerk Maxwell Building,
Mayfield Road, Edinburgh, EH9 3JZ UK

October 6, 2011

Abstract

Singlet and triplet vertical excitation energies from time-dependent density functional theory (TDDFT) can be affected in different ways by the inclusion of exact exchange in hybrid or Coulomb-attenuated/ range-separated exchange–correlation functionals; in particular, triplet excitation energies can become significantly too low. To investigate these issues, the explicit dependence of excitation energies on exact exchange is quantified for four representative molecules, paying attention to the effect of constant, short-range, and long-range contributions. A stability analysis is used to verify that the problematic TDDFT triplet excitations can be understood in terms of the ground state triplet instability problem and it is proposed that a Hartree–Fock stability analysis should be used to identify triplet excitations for which the presence of exact exchange in the TDDFT functional is undesirable. The use of the Tamm–Dancoff approximation (TDA) significantly improves the problematic triplet excitation energies, recovering the correct state ordering in benzoquinone; it also affects the corresponding singlet states, recovering the correct state ordering in naphthalene. The impressive performance of the TDA is maintained for a wide range of molecules across representative functionals.

1   Introduction

Time-dependent[1–4] density functional theory[5–8] (TDDFT) in the adiabatic approximation is a widely-used method for studying molecular electronic excited states. The accuracy of a TDDFT calculation is largely governed by the choice of exchange–correlation functional. Generalised gradient approximations (GGAs) have been largely superseded by hybrid functionals that incorporate a fixed amount of exact orbital exchange (hereafter denoted exact exchange), independent of the inter-electron distance r_{12}. [Exact exchange in the DFT context is defined as the standard Hartree–Fock (HF) exchange energy expression, evaluated using the Kohn–Sham orbitals.] More recently, there has been enormous growth in the use of so-called Coulomb-attenuated or range-separated functionals[9–18] where the amount of exact exchange depends on r_{12}. The primary reason for this growth is that functionals where the amount of exact exchange increases with r_{12} have been shown to yield notably improved long-range, Rydberg and charge-transfer excitation energies, whilst maintaining good quality local excitations.[12,14,16,17,19–26] The majority of these studies have considered excitations to singlet excited states. The quality of excitations to triplet states with Coulomb-attenuated/ range-separated functionals, of technological importance in phosphorescence in OLEDs, bioimaging, etc., is less well documented.[27–29]

Recent work by Thiel and co-workers[30–32] has provided a set of correlated wavefunction [complete active space self-consistent field with second order perturbation theory (CASPT2) and linear response coupled cluster with approximate perturbative triple excitations[33] (CC3)] benchmark results on small, closed-shell organic molecules, allowing comparison of low-lying local singlet and triplet vertical excitation energies within the same molecule. Amongst others, Silva-Junior[34] *et al.*, Jacquemin[23,27] *et al.*, Della Sala and Fabiano,[35] and Huix-Rotllant[36] *et al.* have assessed the performance of various DFT-based methods for this set. We have repeated the conventional TDDFT calculations of Refs. 23,27 and 34, using the aug-cc-pVTZ basis set (which, unless otherwise stated, is used throughout this study), with the PBE[37] (GGA, no exact exchange), B3LYP[38–43] (hybrid, fixed 20% exact exchange), and CAM-B3LYP[12] (Coulomb-attenuated, with 19% exact exchange increasing with r_{12} to 65%) functionals at the same MP2/ 6-31G* geometries. We consider 63 vertical triplet excitations and the 57 equivalent vertical singlet excitations for which reference CASPT2/ CC3 reference values are available, using the Dalton[44] and Gaussian 09[45] programs. Mean and mean absolute errors, relative to the reference values, are presented as blue bars in Figure 1.

The results for the singlet states illustrate the well-known trend: The PBE GGA functional underestimates the excitation energies, whilst increasing the amount of exact exchange (PBE $\rightarrow$ B3LYP $\rightarrow$ CAM-B3LYP) beneficially increases the excitation energies, reducing mean and mean absolute errors. For triplet states, PBE again underestimates the excitation energies, but the improvement upon increasing the amount of exact exchange is much less pronounced than for the singlet states. The reason for this different behaviour is evident from an analysis of individual excitations—whilst in many cases the triplet excitation energy does (beneficially) increase with increasing exact exchange, in many other cases it *drops* significantly, leading to a degradation in accuracy. The latter behaviour is not a consequence of low-overlap charge-transfer[20] failure.

It has long been known[46–53] that time-dependent Hartree–Fock theory (TDHF, 100% exact exchange) significantly underestimates triplet excitation energies when there is a triplet instability problem in the ground state wavefunction and that this underestimation can be largely overcome using configuration interaction singles (CIS). Given the similarity between the TDDFT and TDHF formalisms, we should anticipate similar problems in TDDFT, particularly as the amount of exact exchange increases, which could explain the observed underestimation of certain states. Bauernschmitt and Ahlrichs[49] and Hirata and Head-Gordon[54] presented early examples where hybrid functionals underestimate triplet excitation energies in systems known to have triplet instability problems. The latter authors also demonstrated that these errors are largely eliminated upon application of the Tamm–Dancoff approximation,[55,56] which is the TDDFT analogue of CIS.

In the present study, we explicitly quantify the influence of exact exchange on representative TDDFT singlet and triplet excitation energies and verify that the problematic triplet states can be understood in terms of the triplet instability problem. Despite being highlighted in several studies,[49,54,57–59] this consequence of triplet instabilities is not widely appreciated in the TDDFT user community; it is, however, of increasing relevance due to the growth in the use of functionals containing large amounts of exact exchange. We propose that a stability analysis of the Hartree–Fock wavefunction should be used to identify triplet excitations for which the presence of exact exchange in the TDDFT functional is undesirable. By analogy with the TDHF/ CIS case, and following Ref. 54, we then quantify the extent to which the TDDFT triplet problems can be overcome using the Tamm–Dancoff approximation. We also consider the effect of this approximation on singlet states, including state ordering in naphthalene, which is a challenging problem for approximate TDDFT. Finally, the full error analysis in Figure 1 is repeated using the Tamm–Dancoff approximation.

We commence in Section 2 by quantifying the influence of exact exchange on singlet and triplet excitation energies for a representative set of molecules. Section 3 relates the observations to the triplet instability and Section 4 considers the Tamm–Dancoff approximation. Conclusions are presented in Section 5.

2   Exchange dependence of excitation energies

To illustrate and quantify the influence of exact exchange in a systematic manner, we first consider the evolution of vertical excitation energies as a function of the fraction of exact exchange in a conventional global hybrid functional. Following Becke,[60] we define

$$E_{xc} = \alpha E_x^{HF}[\varphi] + (1 - \alpha)E_x^{B}[\rho, \nabla\rho] + E_c^{LYP}[\rho, \nabla\rho], \qquad (1)$$

where the notation $[\varphi]$, $[\rho]$, and $[\nabla\rho]$ indicates explicit orbital, density, and density gradient dependence, respectively; B represents Becke's 1988[39] gradient corrected exchange functional combined in equal proportions with Dirac/ Slater[61,62] LDA exchange, and LYP represents the Lee–Yang–Parr[40] GGA correlation functional. From the benchmark set of Thiel and co-workers,[32] we consider four representative molecules: ethene, E-butadiene, p-benzoquinone and naphthalene, using the same geometries as before. Additional results for formaldehyde and formamide are presented in the supplementary material. To facilitate comparison with previous studies, we adopt the molecular orientation (and hence symmetry labels) of the earlier works.

In each of Figures 2–5, the left panel shows singlet excitation energies, whilst the right panel shows the equivalent triplet excitation energies (i.e., those that involve pre-

4

dominantly the same orbital transitions), as a function of the fraction of exact exchange α in Eq. (1). The lighter solid line of each colour represents conventionally evaluated TDDFT excitation energies, to be compared with the horizontal dashed lines that represent accurate reference values, taken from Ref. 32. For ethene, values were not available for all of the states we consider; comparison is instead made with the experimentally derived reference values used in Ref. 63, and the d-aug-cc-pVTZ basis set is used for the calculations. In all cases, the GGA ($\alpha = 0$) singlet and triplet excitation energies underestimate the respective reference values.

First consider ethene in Figure 2. As α increases, both of the singlet excitation energies increase and each becomes more accurate (albeit at the expense of a less accurate relative energy). For the $^3B_{3u}$ state, the variation with α is nearly identical to the singlet transition; a significant amount of exact exchange is again optimal. By contrast, the $^3B_{1u}$ state demonstrates markedly different behaviour; the excitation energy becomes significantly less accurate with increasing α, as it *drops* by nearly 2 eV between $\alpha = 0$ and $\alpha = 1$.

For butadiene in Figure 3, both of the singlet excitation energies again increase with α, with notably different optimal values. However, both of the triplet excitation energies drop in energy, with each becoming significantly less accurate as α increases. The ^3A_g energy drops by over 1 eV whilst the ^3B_u energy drops considerably more, eventually yielding an imaginary excitation energy (we only plot the real excitation energies).

Next, consider benzoquinone in Figure 4, where three states of each spin are considered. All three singlet excitation energies increase at a similar rate with α, with modest amounts of exact exchange providing optimal results. By contrast, the three triplet states each exhibit a different dependence on α. The $^3B_{1g}$ energy behaves essentially identically to the singlet counterpart; the $^3B_{3g}$ energy decreases, becoming less accurate; whilst the $^3B_{1u}$ energy drops rapidly, becoming imaginary for large α. This differential dependence means that the triplet state ordering is sensitive to the value of α. The GGA calculation correctly places the $^3B_{1g}$ state lowest in energy, but the ordering becomes incorrect as α increases, with first the $^3B_{1u}$ state and then the $^3B_{3g}$ state dropping below the $^3B_{1g}$.

Finally, consider naphthalene in Figure 5, where the B_{2u} and B_{3u} states correspond to the L_a and L_b states in the usual Platt notation. Both of the singlet excitation energies increase in energy with α, although no value of α yields the correct ordering of the two states. This is a well-known problem in approximate TDDFT.[20,64–68] For the triplet states, the $^3B_{3u}$ excitation energy increases gradually with α and is accurately described, whereas the $^3B_{2u}$ excitation energy decreases dramatically and becomes imaginary for large α.

The results in Figures 2–5 were obtained using a global hybrid functional, where

the amount of exact exchange is independent of r_{12}. In order to ascertain the relative importance of the long- and short-range components of the exact exchange on the six identified 'dropping' triplet states, we have performed additional calculations using Coulomb-attenuated/ range-separated analogues of Eq. (1). For the long-range calculations, we considered a series of functionals with zero exact exchange at short r_{12}, increasing to α exact exchange at large r_{12}. For the short-range calculations, we considered a series with α exact exchange at short r_{12}, decreasing to zero exact exchange at large r_{12}. Both functionals used a standard error function partitioning with attenuation parameter $\mu = 0.33$ bohr^{-1}. In all cases, the variation in excitation energy as a function of α is smooth and monotonic. For the long-range functionals, the changes in excitation energies between $\alpha = 0$ and $\alpha = 1$ are -0.23, -0.22, -0.23, -0.17, $+0.15$ and -0.20 eV, for ethene ($^3B_{1u}$), butadiene (^3B_u and ^3A_g), benzoquinone ($^3B_{1u}$ and $^3B_{3g}$), and naphthalene ($^3B_{2u}$) respectively. For the short-range functionals, the changes are more pronounced, at -1.48, -1.59, -0.93, -2.49 (imaginary beyond that point), -0.68 and -1.50 eV. We conclude that long-range and short-range exact exchange each tend to cause these triplet excitation energies to decrease, with the effect of the latter (unsurprisingly) being more pronounced.

From this analysis, we would predict that both B3LYP (fixed exact exchange) and CAM-B3LYP (fixed- and long-range exact exchange) should both underestimate the same six triplet excitation energies and we have verified that this is indeed the case; mean errors are -0.51 eV and -0.64 eV, respectively (compared to -0.38 eV with PBE). The same would be true for any other molecule in the benchmark set where exact exchange causes the triplet excitation energy to drop. To understand why some, but not all, triplet excitation energies drop with exact exchange, we must consider the influence of the triplet instability on TDDFT results.

3 The triplet instability problem

The triplet instability in Hartree–Fock theory is well-known.[46,69] Figure 6(a) presents potential energy curves for the prototypical molecule, H_2. The $^1\Sigma_g^+$ spin-restricted Hartree–Fock (RHF) ground state energy becomes too high as the internuclear distance R increases, due to unphysical ionic components in the wavefunction. The repulsive $^3\Sigma_u^+$ unrestricted Hartree–Fock (UHF) state does not contain any unphysical ionic components and so dissociates correctly. Consequently, instead of the $^3\Sigma_u^+$ and $^1\Sigma_g^+$ states becoming degenerate at large R, the energy of the $^3\Sigma_u^+$ state drops below that of the $^1\Sigma_g^+$ for R larger than ~ 3 bohr. Also shown is the UHF ground state solution, which allows mixing of triplet state character into the singlet wavefunction. The UHF energy drops below the RHF energy beyond the Coulson–Fischer (CF)[70] point (~ 2.3 bohr in

H_2) and correct dissociation is obtained. The RHF solution is therefore unstable with respect to spin-symmetry breaking.

Computationally, this triplet instability manifests as a negative eigenvalue in the electronic Hessian, indicating that specific orbital rotations of an identified space–spin symmetry will lower the energy. Henceforth we refer to the eigenvalues of this matrix as 'stability measures'. Figure 6(b) presents the lowest $^3\Sigma_u^+$-symmetry stability measure of the Hartree–Fock wavefunction for H_2, as a function of R. It reduces to zero at the CF point and becomes negative beyond. [The stability measures associated with a single determinant are simple to compute and can for instance be calculated in Gaussian[45] using the `stable` keyword, where IOp(9/41) controls the number computed.]

There are intrinsic similarities[49,52] between the equations used to determine the stability and the TDHF/TDDFT equations and so triplet instabilities have significant implications for excited states determined using these methods. The eigenvectors of the electronic Hessian have identifiable analogues amongst the orbital rotations associated with electronic excitations and so it is generally possible to associate a stability measure with each excitation; the stability measure in Figure 6(b) corresponds to the lowest $^1\Sigma_g^+ \rightarrow {}^3\Sigma_u^+$ excitation. Figure 6(c) presents this excitation energy as a function of R. The exact excitation energy approaches zero as $R \rightarrow \infty$. The 'ΔSCF' curve, obtained from the energy difference between the potential energy curves in Figure 6(a), becomes increasingly negative at large R, reflecting the significant overestimation of the $^1\Sigma_u^+$ energy. The influence of the triplet instability on the TDHF excitation energies is striking. The values are reasonable for small R but as the CF point is approached, the values become increasingly underestimated, reaching zero at the CF point and becoming imaginary beyond. Analogous results (in the DFT context) have been presented by Casida *et al.*[57]

The unphysical TDHF excitation energies obtained for large R are exacerbated by the fact that whilst ground state HF theory is variational, TDHF is not; for an arbitrary state the TDHF total electronic energy is no longer a rigorous upper bound on the exact energy. A simple way to restore the variational nature of the excited state energies is to use configuration-interaction singles (CIS) instead of TDHF theory. Figure 6(c) shows that the CIS excitation energies are close to those from ΔSCF. The excitation energies become negative at large R, rather than imaginary, due to the Hermitian nature of the CIS matrix equations (see Section 4).

The key result of this analysis is that as the triplet stability measure decreases towards zero, so the corresponding time-dependent triplet excitation energy also approaches zero, thereby increasingly underestimating the exact value; when the stability measure becomes negative (i.e., when there is a triplet instability), the excitation energy becomes imaginary. By contrast, CIS is much less problematic. Returning to the

TDDFT results in Figures 2–5, we have determined DFT stability measures for the $\alpha = 0$ and $\alpha = 1$ functionals for each of the triplet excitations; results are presented in Table 1. For the two states that (beneficially) increase significantly in energy with α, the stability is large and increases between $\alpha = 0$ and $\alpha = 1$. For the one state whose energy is approximately independent of the amount of exact exchange, the stability varies only slightly. For the three states that drop in energy, but do not become imaginary, the stability reduces significantly. For the three states whose energy drops and becomes imaginary, the stability again reduces significantly, and becomes negative by $\alpha = 1$. The fact that the dropping triplets are associated with a significant reduction in the stability indicates that the drop—and the resultant underestimation from functionals such as B3LYP and CAM-B3LYP—can be understood in terms of the ground state triplet instability problem, consistent with Refs. 49 and 54. Analogous results for formaldehyde and formamide are presented in the Supplementary Material. We note that an alternative explanation for the underestimated triplet state energies in ethene was recently proposed by Cui and Yang[28].

Given that it is the inclusion of exact exchange that exacerbates the triplet instability problem, it is also pertinent to calculate the stabilities of these states for the Hartree–Fock wavefunction. Results are presented in Table 1 and the trend closely follows that of the $\alpha = 1$ DFT results. [We have confirmed that in cases where the Hartree–Fock stability is large (> 2 eV), TDHF and CIS yield similar triplet excitation energies; when the stability is small but positive, TDHF excitation energies are notably smaller than CIS; when the stability is negative, TDHF excitation energies are imaginary, whilst the CIS values remain real.] This leads us to recommend that a Hartree–Fock stability analysis be undertaken when computing triplet excitations, to identify states for which the presence of exact exchange in the TDDFT functional is undesirable: The analysis in Table 1 and the supplementary material (albeit on a limited number of molecules) suggests that in cases where the Hartree–Fock stability is less than ~ 2 eV, the inclusion of exact exchange in the functional will lead to a decrease in excitation energy. If GGAs underestimate the triplet excitation energy (as they often do), then such a decrease will be detrimental. Of course, one could alternatively determine the stability of the DFT calculation directly, but test calculations suggest that the molecule-dependent amount of exact exchange introduced by Coulomb-attenuated/ range-separated functionals yields a less-well defined threshold.

4 The Tamm–Dancoff approximation in TDDFT

The CIS approximation corresponds to setting $\mathbf{B} = \mathbf{0}$ in the TDHF generalized eigenvalue equations

$$\begin{pmatrix} \mathbf{A} & \mathbf{B} \\ \mathbf{B} & \mathbf{A} \end{pmatrix} \begin{pmatrix} \mathbf{X} \\ \mathbf{Y} \end{pmatrix} = \omega \begin{pmatrix} \mathbf{1} & \mathbf{0} \\ \mathbf{0} & -\mathbf{1} \end{pmatrix} \begin{pmatrix} \mathbf{X} \\ \mathbf{Y} \end{pmatrix} \tag{2}$$

which is known as the Tamm–Dancoff[55,56] approximation (TDA) to TDHF. The TDDFT equations take exactly the same form (with different matrices $\mathbf{A}$ and $\mathbf{B}$[52]) and so the TDA can equivalently be applied[54] to TDDFT by setting $\mathbf{B} = \mathbf{0}$; see Ref. 71 for an earlier, related concept. Physically, the TDA corresponds to allowing only excitation between occupied–virtual orbital pairs (given by the eigenvector $\mathbf{X}$) as opposed to conventional TDHF/ TDDFT, where virtual–occupied de-excitation contributions ($\mathbf{Y}$) are also allowed. The form of the TDA eigenvalue equation precludes the occurrence of imaginary excitation energies since $\mathbf{A}$ is Hermitian. We note that there is sometimes concern[52] regarding the validity of transition intensities (oscillator strengths) computed from calculations involving the TDA as they do not satisfy the Thomas–Reiche–Kuhn sum-rule.[72–74] However, this is of no relevance to the calculation of non spin-orbit coupled triplet transitions and we therefore do not consider its implications in this study. The TDA is often used as an approximation to full TDDFT due to its relative computational simplicity. Results are often in excellent agreement with full TDDFT (the discrepancy is usually considerably smaller than between CIS and TDHF), but there are instances where TDA yields a better model of reality[53,54,58,66,75]

Given that CIS is a significant improvement over TDHF when there is a failure associated with triplet instability problems, we now quantify the extent to which the TDA fixes the problematic TDDFT excitations of Section 2. We return to Figures 2–4, and now consider the dark solid lines which present results for TDA excitation energies, as a function of the amount of exact exchange α. We use the NWChem 6.0 program[76] for the calculation of TDA excitation energies.

First consider ethene in Figure 2. The use of the TDA leads to a significant increase and improvement in the problematic $^3B_{1u}$ excitation energies. By contrast, the $^3B_{3u}$ excitation energies barely change. Notably, the TDA also leads to a shift by about $+0.5$ eV in the $^1B_{1u}$ state energy—the singlet analogue of the problematic triplet state— resulting in a significant improvement. The $^1B_{3u}$ state is barely affected.

For butadiene in Figure 3, the TDA leads to a significant increase in both of the problematic triplet states, greatly improving accuracy. The improvement is most pronounced for the ^3B_u state, which was the most problematic. As with ethene, the corresponding singlet state energy is notably shifted and improved, whilst the ^1A_g state is less affected.

For benzoquinone in Figure 4, the effect of the TDA again increases as the triplet instability problem becomes more severe from $^3B_{1g}$ to $^3B_{2g}$ to $^3B_{1u}$, leading to the correct state ordering for small values of α; the singlet states are again shifted to higher energy by proportionate amounts.

Finally, analogous observations are also made for naphthalene in Figure 5. The TDA leads to a dramatic improvement in the problematic triplet state. Significantly, the associated shift in the corresponding singlet state fixes the state ordering for most values of α (although the energy difference remains poor), consistent with Ref. 66. This suggests that the origin of the incorrect state ordering is related to the triplet instability problem associated with the $^3B_{2u}$ state (see Ref. 68 for an alternative discussion). We note that calculations with the CAM-B3LYP functional, which correctly predicts the state ordering with conventional TDDFT (by only 0.02 eV), is able to correctly increase the energy difference between the two states once the TDA is invoked (the difference becomes 0.18 eV).

Consistent with the findings of Ref. 54, the results of Figures 2–5 illustrate the benefit of using the TDA for calculating triplet excitation energies when there is a triplet instability problem. Perhaps less expected is the associated effect/ improvement of the corresponding singlet states. We end this study by returning to the full assessment in Figure 1; we have repeated all calculations using the TDA and the results are presented as green bars. The performance of the TDA is impressive, particularly for the triplet states. Indeed, the only error measure that discernibly degrades is the singlet CAM-B3LYP mean error.

5   Conclusions

In this study, we highlighted the fact that singlet and triplet vertical excitation energies in TDDFT can be affected in different ways by the inclusion of exact exchange in hybrid or Coulomb-attenuated/ range-separated functionals. The improvement upon addition of exact exchange is less pronounced for triplet states, which can be traced to the fact that some triplet excitation energies become significantly too low. We studied the explicit dependence of excitation energies on exact exchange for four representative molecules, illustrating the various behaviours and quantifying the effect of constant, short- and long-range contributions.

We then used the H_2 molecule to illustrate the effect of triplet instabilities on time-dependent excitation energies. As the triplet stability measure associated with an excitation decreases, so the corresponding triplet excitation energy increasingly underestimates the exact value, possibly becoming imaginary. By determining DFT stability measures for the states of interest in the four representative molecules, we verified that

the problematic TDDFT triplets can be understood in terms of the ground state triplet instability problem. We proposed that a Hartree–Fock stability analysis should be carried out to identify triplet excitations for which the presence of exact exchange in the TDDFT functional is undesirable.

We then considered the effect of the Tamm–Dancoff approximation in TDDFT. The use of the TDA significantly improves the problematic triplet states, recovering the correct state ordering in benzoquinone. It also affects the corresponding singlet states, recovering the correct state ordering in naphthalene, which is known to be a significant challenge for approximate TDDFT. The impressive performance of the TDA is maintained for the full assessment set, across representative functionals. We are presently expanding the current work to consider the effect of triplet instabilities and the TDA on singlet and triplet states for the more diverse set of molecules/ excitations of Ref. 20 and for a more diverse set of functionals.

Acknowledgements

Supplementary Material

Supplementary material is available. It contains plots of the exact exchange dependence of selected excitation energies in the formaldehyde and formamide molecules together with a table, listing the same information as Table 1, for these molecules. It also includes a plot of the Hartree–Fock stability measure plotted against the difference between the TDHF and CIS excitation energies for the molecules in Table 1, together with formaldehyde and formamide. Tables containing individual excitation energies for the data presented in Figure 1 are also included. This information is available free of charge via the Internet at http://pubs.acs.org/.

Table 1: Stability measures for the DFT functionals in Eq. (1) with $\alpha = 0$, $\alpha = 1$ and for Hartree–Fock.

Molecule	State	$\alpha = 0$	$\alpha = 1$	HF
Ethene				
	$^3B_{1u}$	3.22	0.81	0.05
	$^3B_{3u}$	6.04	7.30	6.61
Butadiene				
	^3B_u	2.21	−0.16	−0.84
	^3A_g	4.06	1.88	1.16
Benzoquinone				
	$^3B_{1u}$	1.89	−0.84	−1.41
	$^3B_{3g}$	2.21	0.33	−0.30
	$^3B_{1g}$	1.25	2.57	2.40
Naphthalene				
	$^3B_{2u}$	2.24	−0.59	−1.25
	$^3B_{3u}$	3.47	2.99	2.66
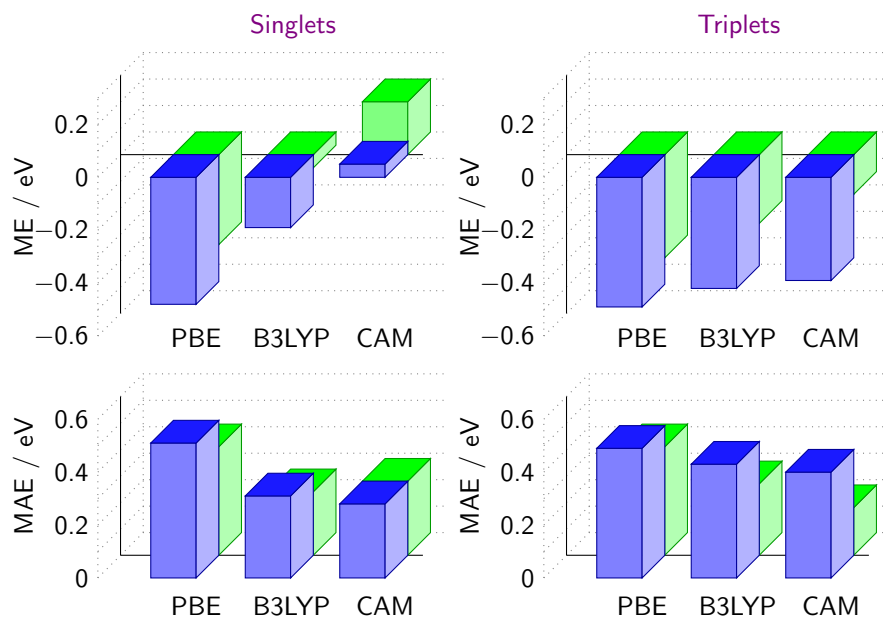
Figure 1: Mean errors (ME) and mean absolute errors (MAE), relative to the reference values of Ref. 32, for 57 singlet and 63 triplet vertical excitation energies. Blue bars represent conventional TDDFT errors; green bars represent TDA errors. CAM denotes CAM-B3LYP.
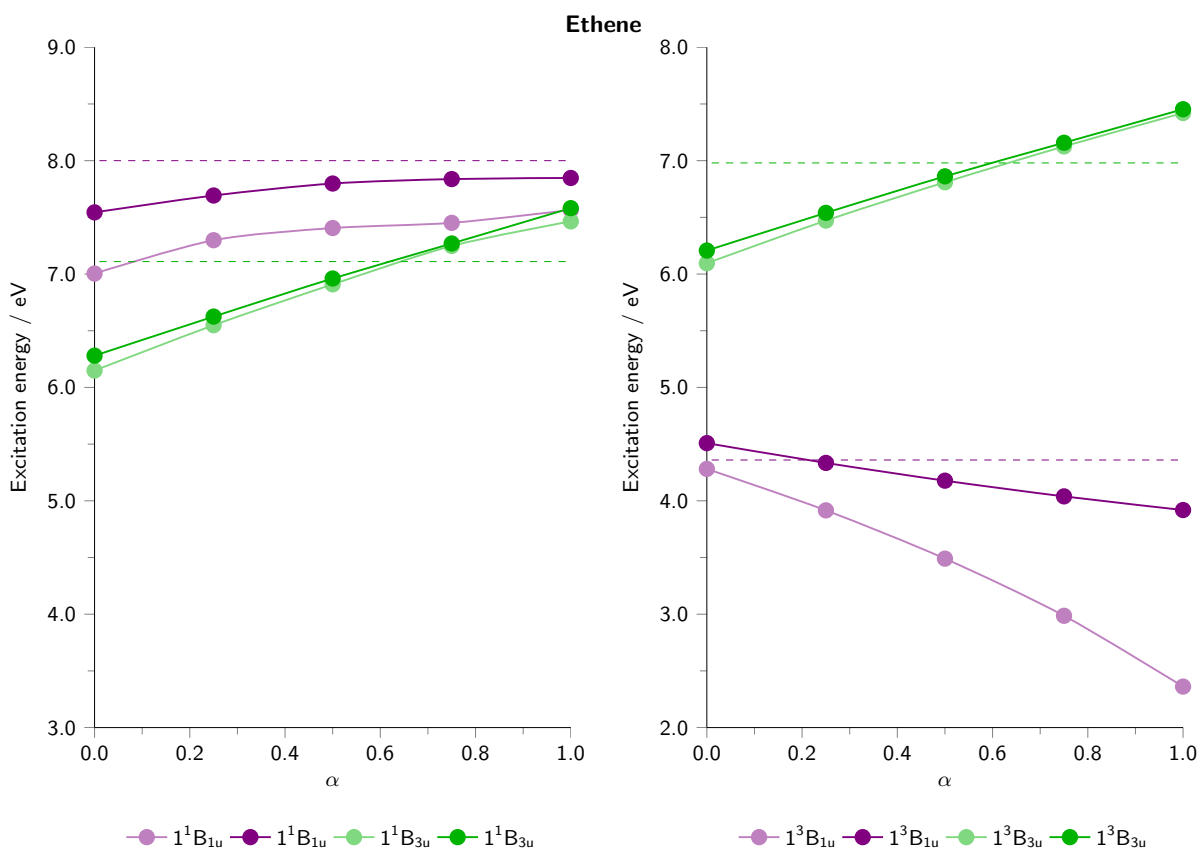
Figure 2: The variation of singlet (left panel) and triplet (right panel) excitation energies in ethene, as a function of the amount of exact exchange α. The lighter version of the colour represents the TDDFT results, the darker version the TDA results. Dashed lines represent reference values.
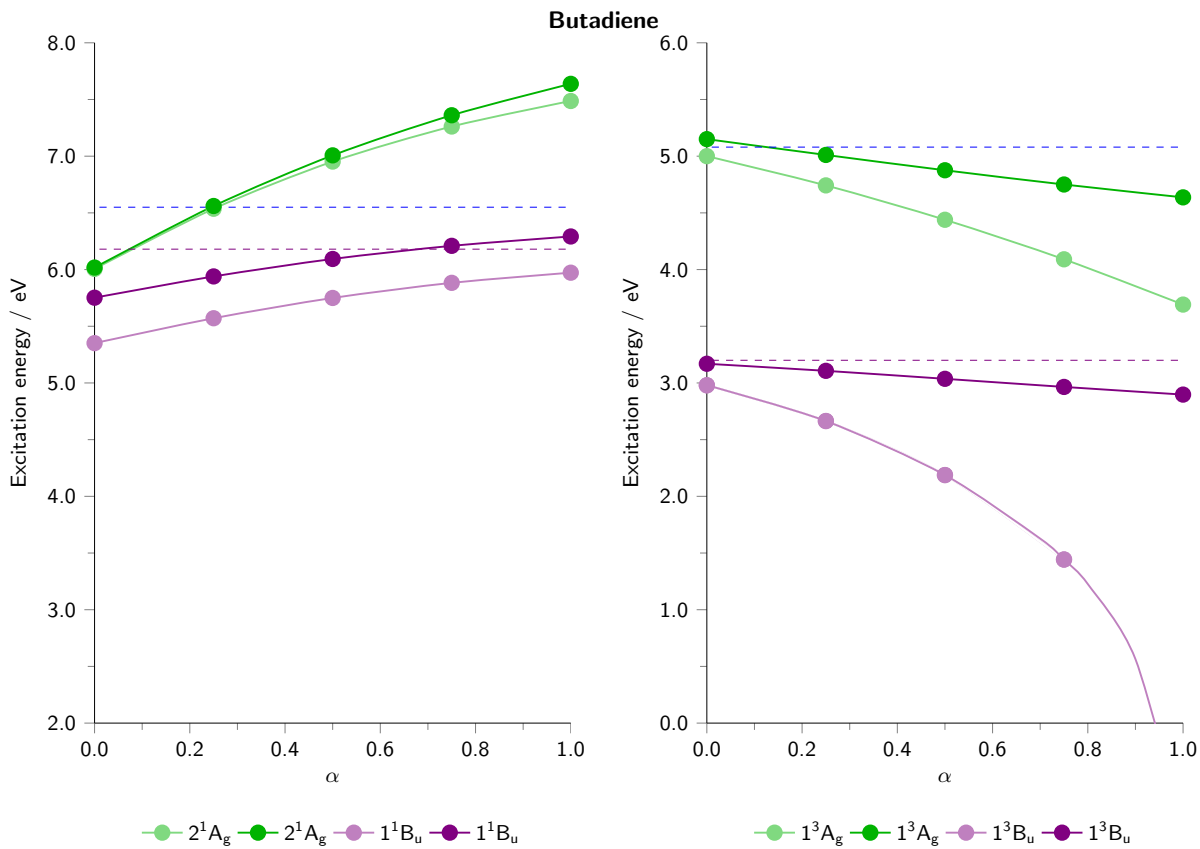
Figure 3: Excitation energies of butadiene; see caption to Figure 2. The TDDFT ^3B_u excitation energy becomes imaginary at large α.
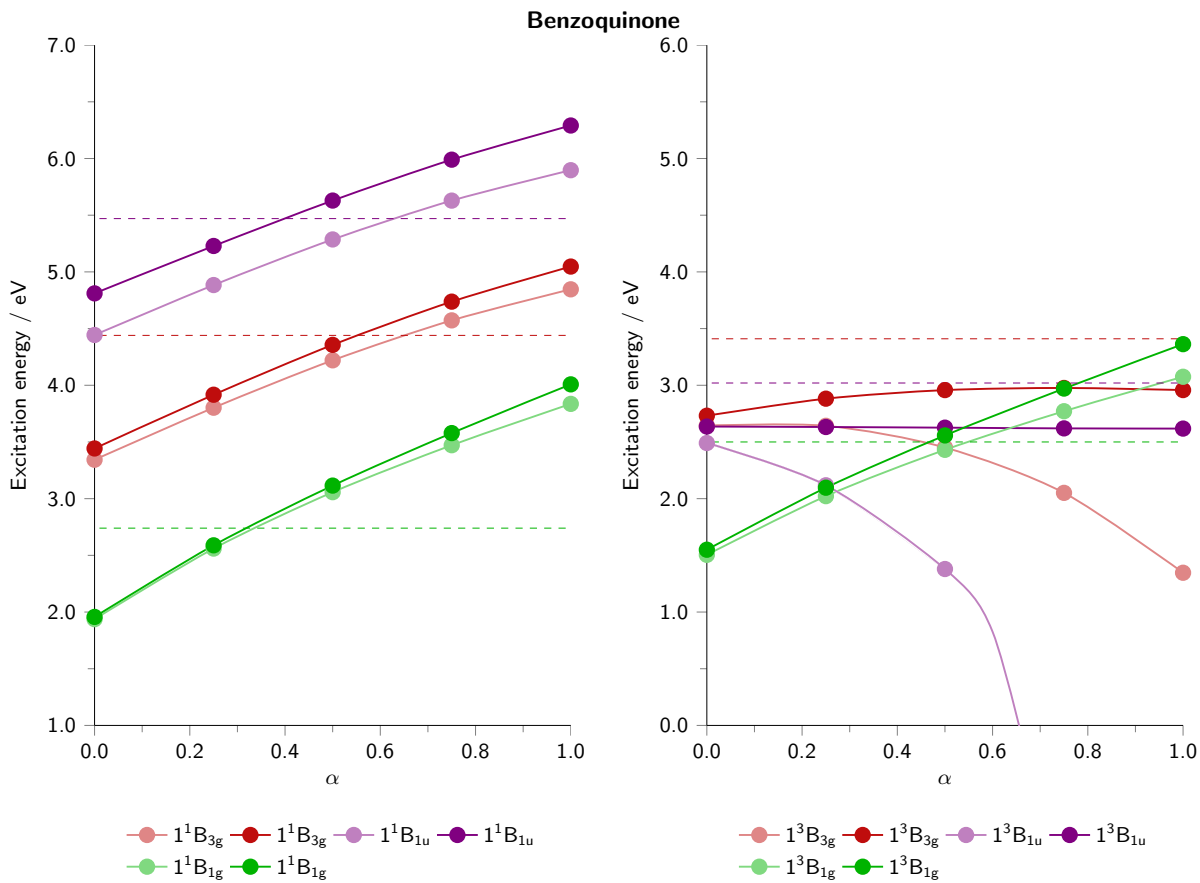
Figure 4: Excitation energies of benzoquinone; see caption to Figure 2. The TDDFT $^3B_{1u}$ excitation energy becomes imaginary at large α
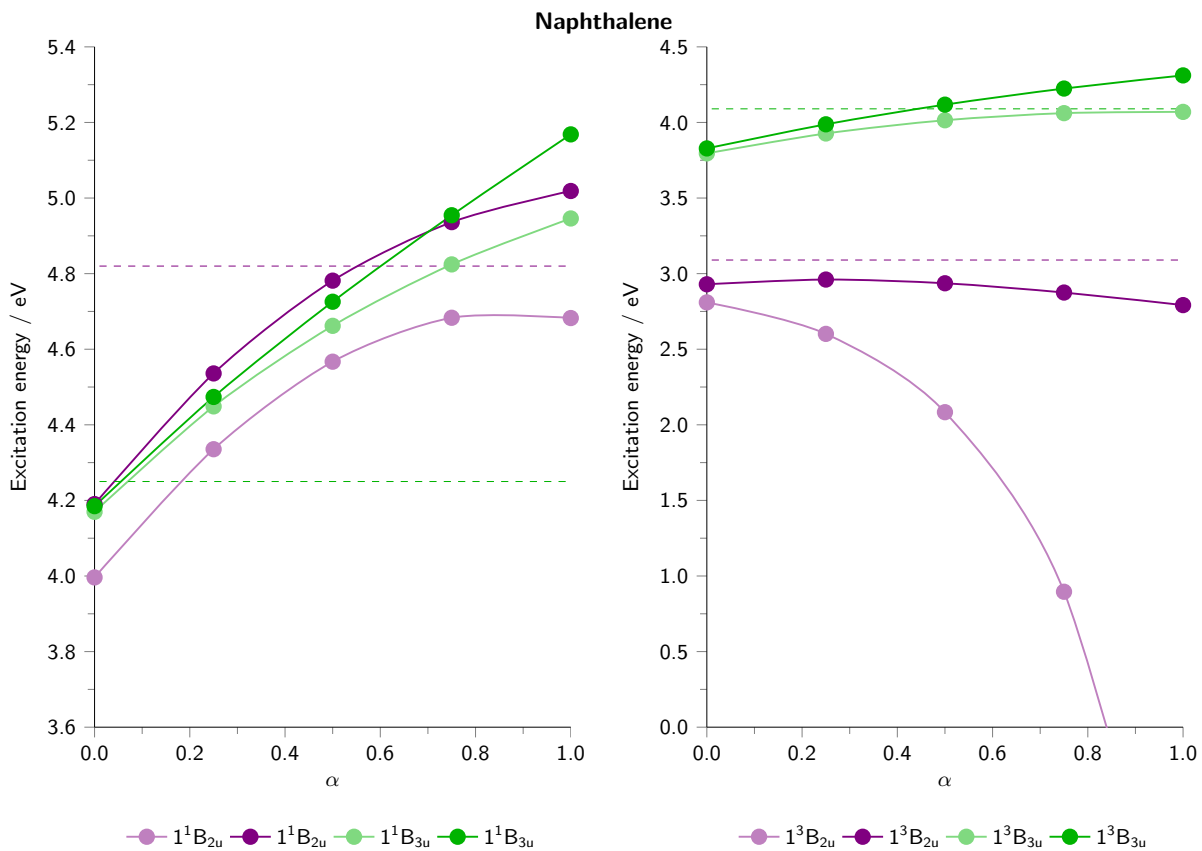
Figure 5: Excitation energies of naphthalene; see caption to Figure 2. The TDDFT $^3B_{2u}$ excitation energy become imaginary at large α. Note that the scale of this figure is different to that of Figures 2–4.
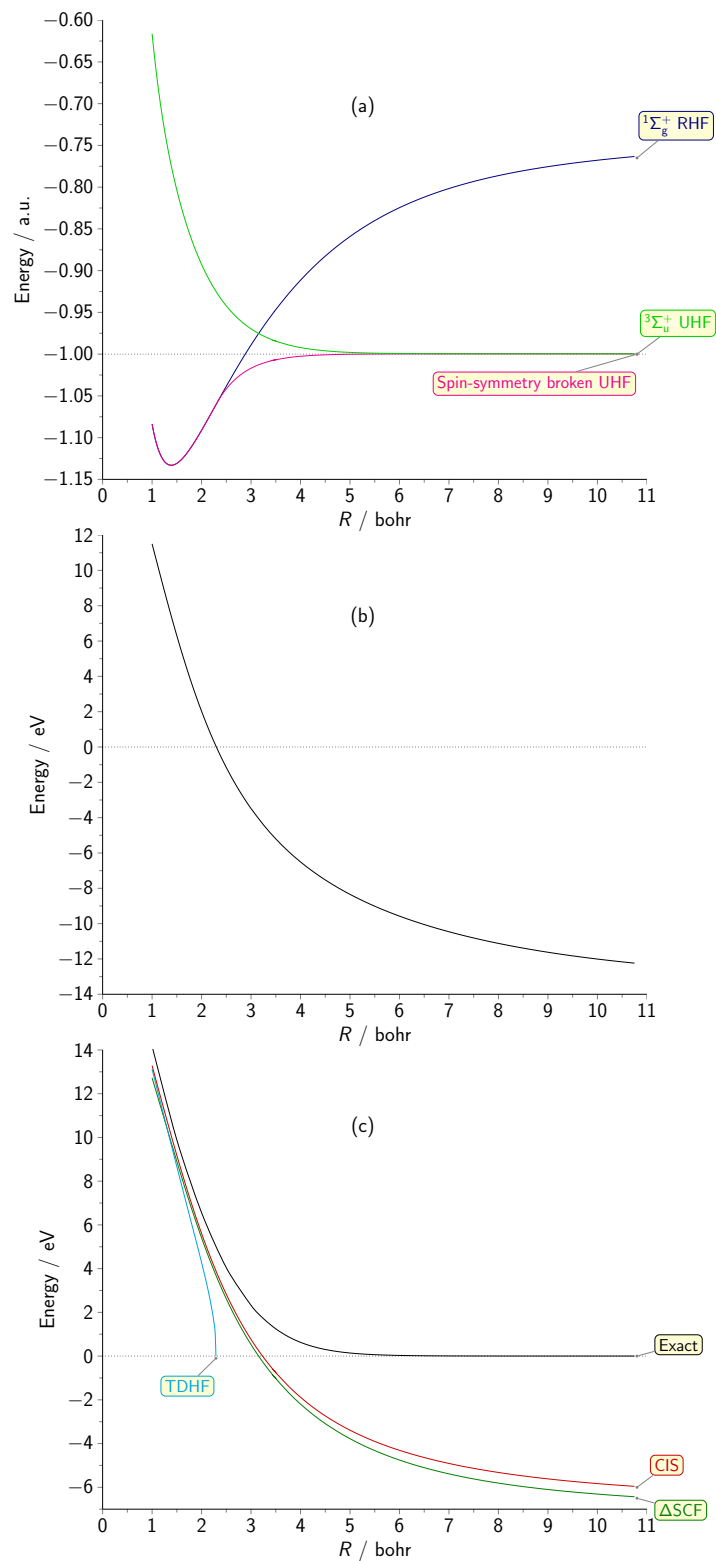
Figure 6: (a) HF electronic energy, (b) HF $^3\Sigma_u^+$ stability measure, and (c) $^1\Sigma_g^+ \rightarrow ^3\Sigma_u^+$ excitation energies, for H_2 as a function of bond length R, using the d-aug-cc-pVTZ basis set.

References

(1) Runge, E.; Gross, E. K. U. *Phys. Rev. Lett.* **1984**, *52*, 997–1000.

(2) Gross, E. K. U.; Ullrich, C. A.; Gossmann, U. J. In *Density Functional Theory*; Gross, E. K. U., Dreizler, R. M., Eds.; NATO ASI Series; Plenum, New York, 1994; pp 149–171.

(3) Casida, M. E. In *Recent Advances in Density Functional Methods, Part I*; Chong, D. P., Ed.; Singapore, World Scientific, 1995; pp 155–192.

(4) Marques, M. A. L.; Gross, E. K. U. In *Time-Dependent Density Functional Theory*; 2003; pp 144–184.

(5) Hohenberg, P.; Kohn, W. *Phys. Rev.* **1964**, *136*, B864–B871.

(6) Kohn, W.; Sham, L. J. *Phys. Rev.* **1965**, *140*, A1133–A1138.

(7) Levy, M. *Proc. Natl. Acad. Sci. USA* **1979**, *76*, 6062–6065.

(8) Parr, R. G.; Yang, W. *Density-Functional Theory of Atoms and Molecules*; International Series of Monographs on Chemistry; Oxford University Press, 1989; pp 142–200.

(9) Gill, P. M. W.; Adamson, R. D.; Pople, J. A. *Mol. Phys.* **1996**, *88*, 1005–1010.

(10) Leininger, T.; Stoll, H.; Werner, H.-J.; Savin, A. *Chem. Phys. Lett.* **1997**, *275*, 151–160.

(11) Iikura, H.; Tsuneda, T.; Yanai, T.; Hirao, K. *J. Chem. Phys.* **2001**, *115*, 3540–3544.

(12) Yanai, T.; Tew, D. P.; Handy, N. C. *Chem. Phys. Lett.* **2004**, *393*, 51–57.

(13) Baer, R.; Neuhauser, D. *Phys. Rev. Lett.* **2005**, *94*, 043002.

(14) Peach, M. J. G.; Cohen, A. J.; Tozer, D. J. *Phys. Chem. Chem. Phys.* **2006**, *8*, 4543–4549.

(15) Vydrov, O. A.; Heyd, J.; Krukau, A. V.; Scuseria, G. E. *J. Chem. Phys.* **2006**, *125*, 074106.

(16) Chai, J.-D.; Head-Gordon, M. *J. Chem. Phys.* **2008**, *128*, 084106.

(17) Rohrdanz, M. A.; Herbert, J. M. *J. Chem. Phys.* **2008**, *129*, 034107.

(18) Besley, N. A.; Peach, M. J. G.; Tozer, D. J. *Phys. Chem. Chem. Phys.* **2009**, *11*, 10350–10358.

(19) Tawada, Y.; Tsuneda, T.; Yanagisawa, S.; Yanai, T.; Hirao, K. *J. Chem. Phys.* **2004**, *120*, 8425–8433.

(20) Peach, M. J. G.; Benfield, P.; Helgaker, T.; Tozer, D. J. *J. Chem. Phys.* **2008**, *128*, 044118.

(21) Peach, M. J. G.; Sueur, C. R. L.; Ruud, K.; Guillaume, M.; Tozer, D. J. *Phys. Chem. Chem. Phys.* **2009**, *11*, 4465–4470.

(22) Jacquemin, D.; Perpète, E. A.; Scuseria, G. E.; Ciofini, I.; Adamo, C. *J. Chem. Theory Comput.* **2008**, *4*, 123–135.

(23) Jacquemin, D.; Wathelet, V.; Perpète, E. A.; Adamo, C. *J. Chem. Theory Comput.* **2009**, *5*, 2420–2435.

(24) Rohrdanz, M. A.; Martins, K. M.; Herbert, J. M. *J. Chem. Phys.* **2009**, *130*, 054112.

(25) Stein, T.; Kronik, L.; Baer, R. *J. Am. Chem. Soc.* **2009**, *131*, 2818–2820.

(26) Peach, M. J. G.; Helgaker, T.; Sałek, P.; Keal, T. W.; Lutnæs, O. B.; Tozer, D. J.; Handy, N. C. *Phys. Chem. Chem. Phys.* **2006**, *8*, 558–562.

(27) Jacquemin, D.; Perpète, E. A.; Ciofini, I.; Adamo, C. *J. Chem. Theory Comput.* **2010**, *6*, 1532–1537.

(28) Cui, G.; Yang, W. *Mol. Phys.* **2010**, *108*, 2745–2750.

(29) Jacquemin, D.; Perpète, E.; Ciofini, I.; Adamo, C. *Theor. Chem. Acc.* **2011**, *128*, 127–136.

(30) Schreiber, M.; Silva-Junior, M. R.; Sauer, S. P. A.; Thiel, W. *J. Chem. Phys.* **2008**, *128*, 134110.

(31) Silva-Junior, M. R.; Sauer, S. P. A.; Schreiber, M.; Thiel, W. *Mol. Phys.* **2010**, *108*, 453–465.

(32) Silva-Junior, M. R.; Schreiber, M.; Sauer, S. P. A.; Thiel, W. *J. Chem. Phys.* **2010**, *133*, 174318.

(33) Christiansen, O.; Koch, H.; Jørgensen, P. *J. Chem. Phys.* **1995**, *103*, 7429–7441.

(34) Silva-Junior, M. R.; Schreiber, M.; Sauer, S. P. A.; Thiel, W. *J. Chem. Phys.* **2008**, *129*, 104103.

(35) Sala, F. D.; Fabiano, E. *Chem. Phys.* **2011**, 10.1016/j.chemphys.2011.05.020.

(36) Huix-Rotllant, M.; Ipatov, A.; Rubio, A.; Casida, M. E. *Chem. Phys.* **2011**, 10.1016/j.chemphys.2011.03.019.

(37) Perdew, J. P.; Burke, K.; Ernzerhof, M. *Phys. Rev. Lett.* **1996**, *77*, 3865–3868.

(38) Becke, A. D. *J. Chem. Phys.* **1993**, *98*, 5648–5652.

(39) Becke, A. D. *Phys. Rev. A* **1988**, *38*, 3098–3100.

(40) Lee, C.; Yang, W.; Parr, R. G. *Phys. Rev. B* **1988**, *37*, 785–789.

(41) Vosko, S. H.; Wilk, L.; Nusair, M. *Can. J. Phys.* **1980**, *58*, 1200–1211.

(42) Stephens, P. J.; Devlin, F. J.; Chabalowski, C. F.; Frisch, M. J. *J. Phys. Chem.* **1994**, *98*, 11623–11627.

(43) We use B3LYP with the VWN5 parameterisation of the local correlation energy.

(44) *Dalton, a molecular electronic structure program, Release Dalton2011*, 2011, see http://daltonprogram.org/ (accessed Oct 2011).

(45) Frisch, M. J.; Trucks, G. W.; Schlegel, H. B.; Scuseria, G. E.; Robb, M. A.; Cheeseman, J. R.; Scalmani, G.; Barone, V.; Mennucci, B.; Petersson, G. A.; Nakatsuji, H.; Caricato, M.; Li, X.; Hratchian, H. P.; Izmaylov, A. F.; Bloino, J.; Zheng, G.; Sonnenberg, J. L.; Hada, M.; Ehara, M.; Toyota, K.; Fukuda, R.; Hasegawa, J.; Ishida, M.; Nakajima, T.; Honda, Y.; Kitao, O.; Nakai, H.; Vreven, T.; Montgomery, J. A., Jr.; Peralta, J. E.; Ogliaro, F.; Bearpark, M.; Heyd, J. J.; Brothers, E.; Kudin, K. N.; Staroverov, V. N.; Kobayashi, R.; Normand, J.; Raghavachari, K.; Rendell, A.; Burant, J. C.; Iyengar, S. S.; Tomasi, J.; Cossi, M.; Rega, N.; Millam, J. M.; Klene, M.; Knox, J. E.; Cross, J. B.; Bakken, V.; Adamo, C.; Jaramillo, J.; Gomperts, R.; Stratmann, R. E.; Yazyev, O.; Austin, A. J.; Cammi, R.; Pomelli, C.; Ochterski, J. W.; Martin, R. L.; Morokuma, K.; Zakrzewski, V. G.; Voth, G. A.; Salvador, P.; Dannenberg, J. J.; Dapprich, S.; Daniels, A. D.; Farkas, Ö.; Foresman, J. B.; Ortiz, J. V.; Cioslowski, J.; Fox, D. J. *Gaussian 09 Revision A.02*, 2009, Gaussian Inc. Wallingford CT 2009.

(46) Seeger, R.; Pople, J. A. *J. Chem. Phys.* **1977**, *66*, 3045–3050.

(47) Foresman, J. B.; Head-Gordon, M.; Pople, J. A.; Frisch, M. J. *J. Phys. Chem.* **1992**, *96*, 135–149.

(48) Jamorski, C.; Casida, M. E.; Salahub, D. R. *J. Chem. Phys.* **1996**, *104*, 5134–5147.

(49) Bauernschmitt, R.; Ahlrichs, R. *J. Chem. Phys.* **1996**, *104*, 9047–9052.

(50) Bauernschmitt, R.; Ahlrichs, R. *Chem. Phys. Lett.* **1996**, *256*, 454–464.

(51) Furche, F.; Ahlrichs, R. *J. Chem. Phys.* **2002**, *117*, 7433–7447.

(52) Dreuw, A.; Head-Gordon, M. *Chem. Rev.* **2005**, *105*, 4009–4037.

(53) Grimme, S.; Neese, F. *J. Chem. Phys.* **2007**, *127*, 154116.

(54) Hirata, S.; Head-Gordon, M. *Chem. Phys. Lett.* **1999**, *314*, 291–299.

(55) Tamm, I. *J. Phys. (USSR)* **1945**, *9*, 449–460.

(56) Dancoff, S. M. *Phys. Rev.* **1950**, *78*, 382–385.

(57) Casida, M. E.; Gutierrez, F.; Guan, J.; Gadea, F.-X.; Salahub, D.; Daudey, J.-P. *J. Chem. Phys.* **2000**, *113*, 7062–7071.

(58) Cordova, F.; Doriol, L. J.; Ipatov, A.; Casida, M. E.; Filippi, C.; Vela, A. *J. Chem. Phys.* **2007**, *127*, 164111.

(59) Lutnæs, O. B.; Helgaker, T.; Jaszuński, M. *Mol. Phys.* **2010**, *108*, 2579–2590.

(60) Becke, A. D. *J. Chem. Phys.* **1993**, *98*, 1372–1377.

(61) Dirac, P. A. M. *Proc. Cam. Phil. Soc.* **1930**, *26*, 376–385.

(62) Slater, J. C. *Phys. Rev.* **1951**, *81*, 385–390.

(63) Tozer, D. J.; Handy, N. C. *J. Chem. Phys.* **1998**, *109*, 10180–10189.

(64) Grimme, S.; Parac, M. *ChemPhysChem* **2003**, *4*, 292–295.

(65) Richard, R. M.; Herbert, J. M. *J. Chem. Theory Comput.* **2011**, *7*, 1296–1306.

(66) Wang, Y.-L.; Wu, G.-S. *Int. J. Quantum Chem.* **2008**, *108*, 430–439.

(67) Wong, B. M.; Hsieh, T. H. *J. Chem. Theory Comput.* **2010**, *6*, 3704–3712.

(68) Kuritz, N.; Stein, T.; Baer, R.; Kronik, L. *J. Chem. Theory Comput.* **2011**, *7*, 2408–2415.

(69) Lee, A. M.; Handy, N. C. *J. Chem. Soc., Faraday Trans.* **1993**, *89*, 3999–4003.

(70) Coulson, C. A.; Fischer, I. *Philos. Mag.* **1949**, *40*, 386–393.

(71) Grimme, S. *Chem. Phys. Lett.* **1996**, *259*, 128–137.

(72) Thomas, W. *Naturwissenschaften* **1925**, *13*, 627–628.

(73) Reiche, F.; Thomas, W. *Z. Phys.* **1925**, *34*, 510–525.

(74) Kuhn, W. *Z. Phys.* **1925**, *33*, 408–412.

(75) Hsu, C.-P.; Hirata, S.; Head-Gordon, M. *J. Phys. Chem. A* **2001**, *105*, 451–458.

(76) Valiev, M.; Bylaska, E.; Govind, N.; Kowalski, K.; Straatsma, T.; Dam, H. V.; Wang, D.; Nieplocha, J.; Apra, E.; Windus, T.; de Jong, W. *Comput. Phys. Commun.* **2010**, *181*, 1477–1489.